

# Investigation of transmission performance in multi-IFoF based mobile fronthaul with dispersion-induced intermixing noise mitigation

MINKYU SUNG,\* SEUNG-HYUN CHO, HWAN SEOK CHUNG, SUN ME KIM,  
AND JONG HYUN LEE

*Department of Optical Internet Research, Electronics and Telecommunications Research Institute, 218, Gajeong Road, Yuseong, Daejeon, 305-700, South Korea*

\*smk9620@etri.re.kr

**Abstract:** We demonstrate the improvement of the transmission performance based on intermixing noise mitigation techniques in a multiple intermediate-frequency-over-fiber (IFoF) based mobile fronthaul. The interaction between fiber chromatic dispersion and frequency chirp of the directly modulated laser generates the second-order distortion that degrades the performance of multi-IFoF transmission system. To avoid second-order distortion, we use intermediate frequency (IF) spacing optimization and octave-confined frequency plan schemes in which intermixing noise would be generated in the out of signal band and would not affect the quality of transmitted signal. For bandwidth efficient transmission of radio signal over mobile fronthaul link, we employ the dispersion compensation technique to suppress the intermixing noise sufficiently. For realization of the multi-IFoF based mobile fronthaul, we experimentally investigate the transmission performances of 48-, 72- and 144-IF carriers of the long term evolution-advanced (LTE-A) signals mapped with 64-quadrature amplitude modulation (QAM). It is clearly observed that the intermixing noise is suppressed owing to dispersion compensation technique and overall system performances are improved by IF spacing optimization and octave-confined frequency plan. As a result, we successfully transmit 144-IF carriers of the LTE-A signal with less than 8% error vector magnitude (EVM) over 20-km single-mode fiber (SMF) within only 3 GHz bandwidth.

© 2017 Optical Society of America

**OCIS codes:** (060.4080) Modulation; (060.0060) Fiber optics and optical communications.

## References and links

1. Framework and Overall Objectives of the Future Development of IMT for 2020 and Beyond, ITU-R, 2015.
2. P. Marsch, I. D. Silva, Ö. Bulakci, M. Tesanovic, S. E. E. Ayoubi, T. Rosowski, A. Kaloylos, and M. Boldi, "5G radio access network architecture: Design guidelines and key considerations," *IEEE Commun. Mag.* **54**(11), 24–32 (2016).
3. C.-L. i, J. Huang, R. Duan, C. Cui, J. X. Jiang, and L. Li, "Recent progress on C-RAN centralization and cloudification," *IEEE Access* **2**, 1030–1039 (2014).
4. A. Checko, H. L. Christiansen, Y. Yan, L. Scolari, G. Kardaras, M. S. Berger, and L. Dittmann, "Cloud RAN for mobile networks—A technology overview," *IEEE Commun. Surv. Tutor.* **17**(1), 405–426 (2015).
5. D. Breuer, E. Weis, K. Grobe, S. Krauß, F. Musumeci, J. T. Gijon, and B. Skubic, "5G transport in future access networks," in *Proceedings of European Conference on Optical Communication* (2016), pp. 229–231.
6. <http://www.cpri.info/>, "Common Public Radio Interface (CPRI); Interface specification" V 6.1, 2014.
7. S. H. Cho, H. Park, H. S. Chung, K. H. Doo, S. Lee, and J. Lee, "Cost-effective next generation mobile fronthaul architecture with Multi-IF carrier transmission scheme," in *Optical Fiber Communication Conference* (2014), paper Tu2B.6.
8. K. Tanaka and A. Agata, "Next-generation optical access networks for C-RAN," in *Optical Fiber Communication Conference* (2015), paper Tu2E.1.
9. K. Miyamoto, S. Kuwano, J. Terada, and A. Otaka, "Analysis of mobile fronthaul bandwidth and wireless transmission performance in split-PHY processing architecture," *Opt. Express* **24**(2), 1261–1268 (2016).

10. B. G. Kim, S. H. Bae, H. Kim, and Y. C. Chung, "Optical fronthaul technologies for next-generation mobile communications," in *Proceedings of International Conference on Transparent Optical Networks* (2017), paper We.D2.6.
11. X. Liu, H. Zeng, N. Chand, and F. Effenberger, "Experimental demonstration of high-throughput low-latency mobile fronthaul supporting 48 20-MHz LTE signals with 59-Gb/s CPRI-equivalent rate and 2- $\mu$ s processing latency," in *Proceedings of European Conference on Optical Communication* (2015), paper We.4.4.3.
12. S. H. Cho, C. Han, H. S. Chung, and J. H. Lee, "Demonstration of mobile fronthaul test bed based on RoF technology supporting two frequency assignments and  $2 \times 2$  MIMO antennas," *ETRI J.* **37**(6), 1055–1064 (2015).
13. S. H. Cho, H. S. Chung, C. Han, S. Lee, and J. Lee, "Experimental demonstrations of next generation cost-effective mobile fronthaul with IFoF technique," in *Optical Fiber Communication Conference* (2015), paper M2J.5.
14. M. Sung, C. Han, S.-H. Cho, H. S. Chung, and J. H. Lee, "Improvement of the transmission performance in multi-IF-over-fiber mobile fronthaul by using tone-reservation technique," *Opt. Express* **23**(23), 29615–29624 (2015).
15. M. Sung, S. H. Cho, K. S. Kim, H. K. Kwon, B. S. Kang, D. S. Oh, D. S. Lyu, H. Lee, S. M. Kim, J. H. Lee, and H. S. Chung, "Demonstration of IFoF based 5G mobile fronthaul in 28 GHz millimeter wave testbed supporting Giga-bit mobile services," in *Optical Fiber Communication Conference* (2017), paper W1C.5.
16. C. Han, M. Sung, S. H. Cho, H. S. Chung, S. M. Kim, and J. H. Lee, "Impact of dispersion-induced second-order distortion in multi-IFoF-based mobile fronthaul link for C-RAN," in *Optical Fiber Communication Conference* (2016), paper TU2B.4.
17. C. Han, M. Sung, S. H. Cho, H. S. Chung, S. M. Kim, and J. H. Lee, "Performance improvement of multi-IFoF-based mobile fronthaul using dispersion-induced distortion mitigation with IF optimization," *J. Lightwave Technol.* **34**(20), 4772–4778 (2016).
18. N. S. André, H. Louchet, K. Habel, and A. Richter, "Analytical formulation for SNR prediction in IMDD OFDM-based access systems," *IEEE Photonics Technol. Lett.* **26**(12), 1255–1258 (2014).
19. G. J. Meslener, "Chromatic dispersion induced distortion of modulated monochromatic light employing direct detection," *IEEE J. Quantum Electron.* **20**(10), 1208–1216 (1984).
20. E. E. Bergmann, C. Y. Kuo, and S. Y. Huang, "Dispersion-induced composite second-order Distortion at 1.5  $\mu$ m," *IEEE Photonics Technol. Lett.* **3**(1), 59–61 (1991).
21. 3GPP TS 36.141 v. 9.8.0, "LTE; Evolved Universal Terrestrial Radio Access (E-UTRA); Base Station (BS) conformance testing," Technical Specification Group Radio Access Network, Rel. 9, July, 2011.
22. N. H. Zhu, T. Zhang, Y. L. Zhang, G. Z. Xu, J. Wen, H. P. Huang, Y. Liu, and L. Xie, "Estimation of frequency response of directly modulated lasers from optical spectra," *J. Phys. D Appl. Phys.* **39**(21), 4578–4581 (2006).
23. 3GPP TS 36.104 v. 11.2.0, "Base Station (BS) Radio Transmission and Reception," Tech. Spec. Group Radio Access Network, Rel. 11, Nov. 2012.

## 1. Introduction

Recently, there has been a lot of interests for 5G mobile communication system to accommodate explosive growth of mobile traffic [1,2]. End to end latency also should be reduced by 1 of 10 than 4G system to meet basic requirements of 5G mobile communication system. Furthermore, many small cell base stations would be densely deployed to offer wide coverage. As an attractive architecture for small cell based radio access networks, the cloud or centralized radio access network (C-RAN) has been introduced owing to superior efficiency in both energy and cost aspects [3–5]. In C-RAN, the digital signal processing unit (DU: digital unit) and remote radio signal processing units (RU: radio unit) are separately operated at the central office and cell sites, respectively. In the DUs, all functions related to digital signal processing are centralized. On the other hand, the RUs carry out simple roles such as signal amplification and frequency conversion. As a result, implementation cost and complexity to construct small cell based networks are significantly reduced. Until now, the network between DUs and RUs, which is so called mobile fronthaul, is usually implemented by using digital optical communication method carrying the common public radio interface (CPRI)-formatted signals. CPRI-based mobile fronthaul has many advantages including simplified compensations and operations in 4G RANs. However, the digitization procedure of radio frequency (RF) signals for CPRI-formatted frame requires very large transmission bandwidth [6]. For example, the required line data-rate of the CPRI-formatted signal is higher than 59 Gb/s to support mobile fronthaul networks of long term evolution-advanced (LTE-A) service exploiting 20-MHz, 2 carrier aggregations (CA), 3 sectors, and 4x4 multiple-input multiple-output (MIMO) system [7]. Besides, the required line data-rate should be explosively

increased by rapid evolution of mobile communication system. Consequently, the CPRI-based mobile fronthaul would be in trouble in terms of implementation cost and complexity aspects.

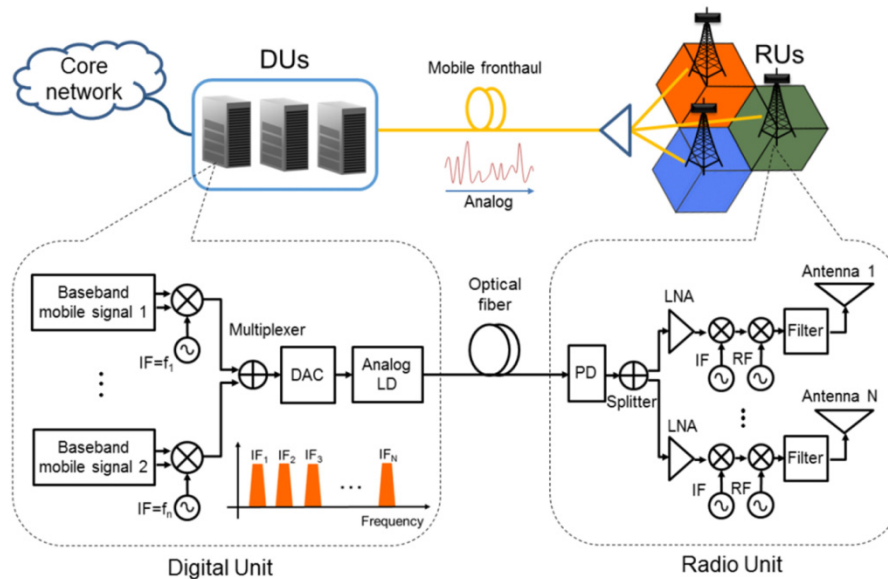


Fig. 1. Configuration of the next-generation mobile fronthaul based on the multi-IFoF technology.

There have been substantial efforts to address fronthaul link's transport capacity requirement, such as CPRI compression, function split, and analog radio-over-fiber (RoF) [8–11]. Among them, the analog RoF technique based on multiple intermediate frequency over fiber (multi-IFoF) system has been proposed and extensively studied as cost-effective and bandwidth-efficient mobile fronthaul as in Fig. 1 [12–15]. In multi-IFoF system, the modulated baseband mobile signals are mapped onto each IF carriers and multiplexed in the frequency domain, providing flexible and efficient bandwidth utilization. Also, the amount that can accommodate small cells in one fiber can be easily increased by using a wavelength division multiplexing (WDM) configuration where a single wavelength optical carrier can carry on multiple IF carriers. In addition, low-cost directly modulated laser (DML) enables reduce the capital expenditure to construct multi-IFoF based mobile fronthaul.

Despite its attractive advantages, the multi-IFoF transmission system experiences severe performance degradation due to second-order distortions induced by interaction between fiber chromatic dispersion and frequency chirp of directly modulated laser [16–18]. The phase noise due to direct modulation of laser is changed to amplitude noise by chromatic dispersion as the signal transmitted through the optical fiber, which generates intermixing noise after direct-detection. As a result, the intermixing noise would be generated in multi-IF carriers, degrading transmission performance.

In this paper, we theoretically investigate the characteristics of intermixing noise mitigation schemes and experimentally evaluate their performances in multi-IFoF based mobile fronthaul. We present principles of intermixing noise mitigation schemes including IF spacing optimization, octave-confined frequency plan, and dispersion compensation. Using IF spacing optimization and octave mapping, the system performance degradation would be negligible because intermixing noise is generated out of data bearing IF carrier bands. Furthermore, intermixing noise is significantly suppressed using dispersion compensation technique because the interplay between the fiber chromatic dispersion and the chirp of the DML was a linear process before detection in photo-diode. By alleviating the intermixing interference, we successfully achieve an error vector magnitude (EVM) of below 8% for 144-

IF carriers LTE-A signal, which have equivalent data-rate of 178-Gb/s CPRI-formatted signal, within 3-GHz bandwidth after 20-km transmission over single-mode fiber (SMF).

The remainder of this paper is organized as follows. The principles of the intermixing noise mitigation schemes are explained in Section 2. The setup for experiments and the performance of the intermixing noise mitigation schemes are described in Section 3. Finally, Section 4 briefly summarizes our discussion.

## 2. Principles of intermixing noise mitigation schemes in multi-IFoF mobile fronthaul

### 2.1 Dispersion-induced second-order distortion

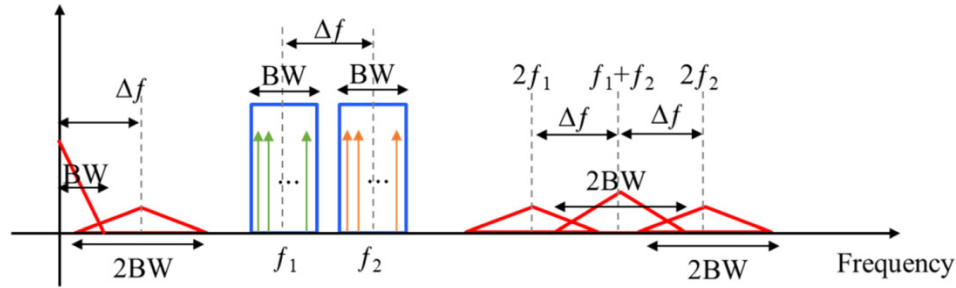


Fig. 2. Second-order distortion components of two IF carriers. The red lines indicate the intermixing noise.

Figure 2 describes the second-order distortion induced by linear interaction between frequency chirp of DML and fiber chromatic dispersion. The intermixing noise occur after photo-detection because the phase noise by direct modulation of laser is changed to amplitude noise by chromatic dispersion as the signal transmitted through the optical fiber, which generates intermixing noise after direct-detection. When the optical modulation index (OMI) is small enough not to cause clipping phenomenon [19], the second-order distortion term predominates and the higher-order distortion terms can be ignored [20]. Therefore, the received optical power applying to the laser a time-dependent current  $I_{bias} + I(t)$  of the laser can be expressed as

$$p' = \alpha \left[ p_{avg} + I(t) \frac{dp}{dI} - \bar{p} \frac{d\Delta\tau}{dt} \right] + \alpha \left[ \frac{I^2(t)}{2} \frac{d^2p}{dI^2} + DL \frac{\lambda^2}{c} \frac{dv}{dI} \frac{dp}{dI} \frac{d(I^2(t))}{dt} \right] \quad (1)$$

where  $\alpha$  is attenuation in optical link,  $p_{avg}$  is the averaged optical power,  $I(t)$  is the modulation current,  $dp/dI$  is the slope efficiency of the laser,  $\Delta\tau$  is the variance of the transit delay with chromatic dispersion,  $d^2p/dI^2$  is the superlinearity intrinsic to the laser,  $D$  is the fiber chromatic dispersion,  $L$  is the length of fiber, and  $dv/dI$  is the frequency chirp [20].  $\lambda$  is the center wavelength of the laser and  $c$  is the speed of light. The first term of the Eq. (1) represent the optical carrier and the desired modulation signal. The second term expresses the second-order distortion induced by the interaction between frequency chirp and fiber dispersion. By converting  $I(t)$  and  $I^2(t)$  into a frequency representation, we can obtain

$$I(t) = \text{Re} \sum_j m_j \cdot e^{i\omega_j t}, \quad I^2(t) = \frac{1}{2} \text{Re} \left( \sum_j \sum_k (m_j \cdot m_k \cdot e^{i(\omega_j + \omega_k)t} + m_j \cdot m_k^* \cdot e^{i(\omega_j - \omega_k)t}) \right) \quad (2)$$

where  $m_j$  is channel amplitude. The spectral power  $P(\omega)$  of a time varying function  $f(t)$  is defined as

$$P(f(t), \omega) = |F(\omega)|^2 \quad (3)$$

Therefore, the spectral power of intermixing noise can be written as

$$\text{Intermixing noise}_{2\text{nd}}(\omega_j \pm \omega_k) = c_j \pm k \cdot m_j^2 \cdot m_k^2 \left\{ \left( \frac{\alpha}{2} \frac{d^2 p}{dI^2} \right)^2 + (\omega_j \pm \omega_k)^2 \left( \alpha DL \frac{dv}{dI} \frac{dp}{dI} \frac{\lambda^2}{c} \right)^2 \right\} \quad (4)$$

From Eq. (4), it can be seen that the intermixing noise is proportional to the square of the frequency and the square of the fiber length.

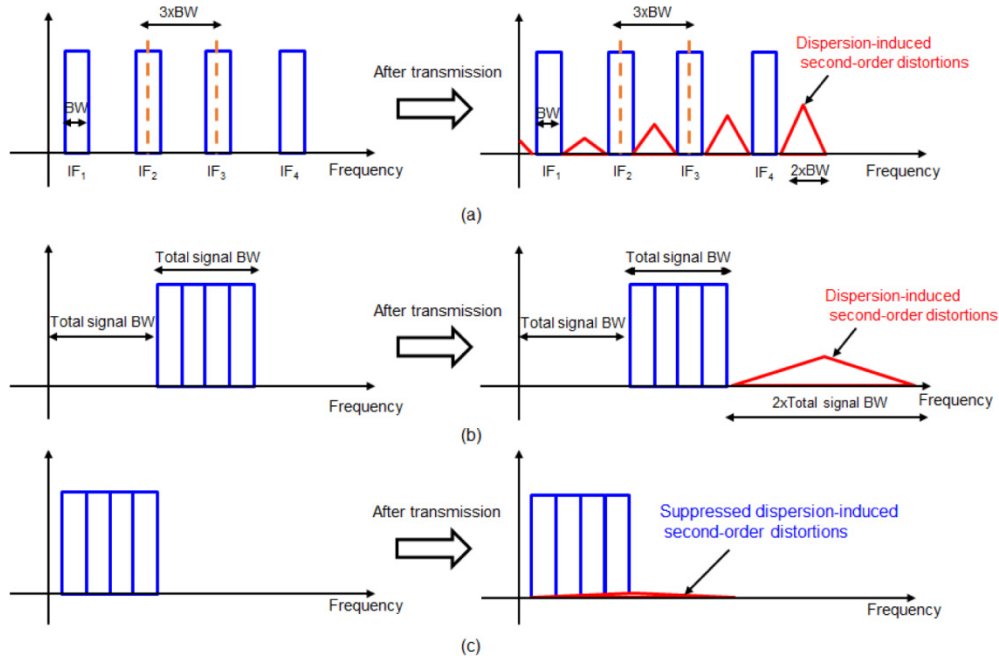


Fig. 3. Concept of intermixing noise mitigation schemes (a) IF spacing optimization, (b) octave-confined frequency plan, and (c) dispersion compensation schemes.

To mitigate the second-order distortion induced by fiber dispersion, we present three schemes of multi-IFoF-based mobile fronthaul link in Fig. 3. The IF spacing optimization and octave-confined frequency plan are able to avoid the intermixing noise using its frequency characteristic as Figs. 3(a) and 3(b). Alternatively, the intermixing noise could be clearly suppressed by compensating dispersion before detection. Since these three schemes are not affected by the signal specification, they could be applied to reduce intermixing noise even if the numerology for 5G mobile signal changes.

### 2.2 Scheme 1: IF spacing optimization

As in Eq. (1), the intermixing noise caused by interplay between frequency chirp of DML and chromatic dispersion dominates to second-order harmonic and intermodulation components. Therefore, we can predict the frequencies at which the second-order distortions appears using IF carrier spacing and initial frequency [17]. Assuming the IF carriers have equal carrier spacing, the frequency ranges of intermixing noise can be expressed as

$$(k-1) \cdot \Delta f - BW < f_{\text{distortion}} < (k-1) \cdot \Delta f + BW, \quad (f_j - f_k \text{ terms, where } k = 1, 2, \dots, n) \quad (5)$$

and

$$2f_1 + (k-1) \cdot \Delta f - BW < f_{\text{distortion}} < 2f_1 + (k-1) \cdot \Delta f + BW, \quad (f_j + f_k \text{ where } k = 1, 2, \dots, 2n-1) \quad (6)$$

From Eq. (1), the IF carriers cannot overlap the distortion components when designing frequency spacing and the initial frequency of IF carriers to be three times the IF carrier bandwidth and odd times of the half carrier spacing, respectively. Figure 3(a) shows the concept of intermixing noise mitigation scheme with IF spacing optimization. It is observed that the crosstalk caused by frequency chirp and fiber dispersion presents after optical fiber transmission. However, intermixing noise is negligible owing to IF spacing optimization in which the crosstalk is located out-of-band between IF carriers. On the other hand, intermixing noise is completely avoided, but loss of spectral efficiency is inevitable. As a result, when IF space optimization technique is used, the spectral efficiency of multi-IFoF system is reduced by a factor of three.

### 2.3 Scheme 2: Octave-confined frequency plan

Figure 3(b) shows the octave-confined frequency plan of IF carriers in which we can avoid the intermixing noise using its frequency characteristic like IF spacing optimization scheme. From Eqs. (5) and (6), we can infer the lowest frequency of the intermixing noise in  $f_j + f_k$  term is  $2f_1 - BW$ , and the highest frequency of the intermixing noise in  $f_j - f_k$  term is  $(n-1) \cdot \Delta f + BW$ . Since the lowest and highest frequency components of transmitted IF signals are  $f_1 - 0.5BW$  and  $f_1 + (n-1) \cdot \Delta f + 0.5BW$ , respectively, we could infer the frequency of IF carriers avoiding the intermixing noise as

$$(n-1) \cdot \Delta f + BW < f_1 - 0.5BW, \quad (f_j - f_k \text{ terms}) \quad (7)$$

and

$$f_1 + (n-1) \cdot \Delta f + 0.5BW < 2f_1 - BW, \quad (f_j + f_k \text{ terms}) \quad (8)$$

When we set the IF spacing is equal as  $\Delta f$ , the total bandwidth could be calculated as

$$\text{Total BW} = (n-1) \cdot \Delta f + BW \quad (9)$$

Therefore, we successfully avoid the intermixing noise in both  $f_j - f_k$  and  $f_j + f_k$  terms by setting the initial center frequency of IF carriers as

$$\text{Total BW} + 0.5BW < f_1 \quad (10)$$

Using octave-confined frequency plan, the intermixing noise are fallen out-of-signal band without interference. The octave-confined frequency plan improve spectral efficiency by about 30% over IF spacing optimization scheme, but it also should experience the spectral efficiency loss.

### 2.4 Scheme 3: Dispersion compensation

Employing schemes 1 and 2, we can completely avoid intermixing noise inducing system degradations, but inevitably suffer spectral efficiency loss. For bandwidth efficient transmission, we use utilize dispersion compensation scheme technique for mobile fronthaul link as in Fig. 3(c). The crosstalk should be significantly suppressed because the interaction between fiber chromatic dispersion and the chirp of the DML was a linear process before direct detection in the photodiode. On the other hand, although the dispersion compensation scheme is excellent in bandwidth efficiency, there is a limit to increase cost and complexity for fronthaul link implementation.

### 3. Experimental setup and results

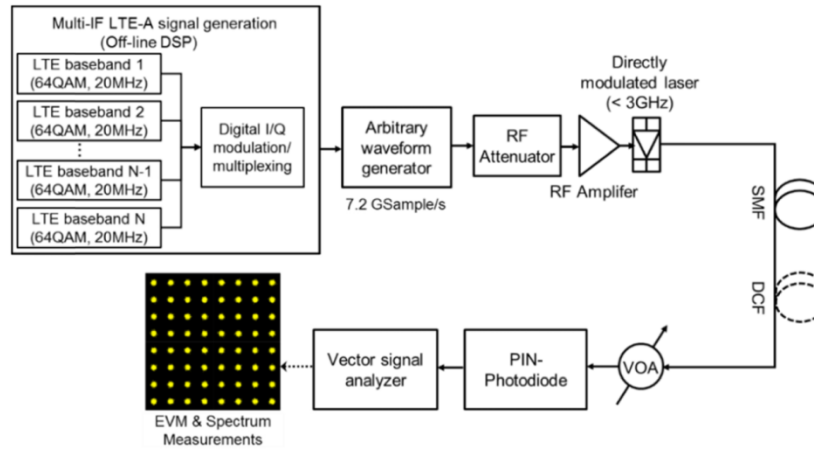


Fig. 4. Experimental setup for multi-IF carrier LTE-A signal transmission over fronthaul link.

In order to verify the feasibility of the intermixing noise mitigation schemes in a multi-IFoF system, we performed a series of experiments on the system described in Fig. 4. We generated multiple LTE-A baseband signals where the each LTE-A baseband signals mapped with 64-quadrature amplitude modulation (QAM), in which each signal had a bandwidth of 20 MHz based on LTE E-UTRA Test Model 3.1. The baseband LTE-A signal is digitally mapped to each IF carrier by digital IQ modulation and multiplexed to simultaneously transmit multiple IF carriers of the LTE-A signals. An arbitrary waveform generator (AWG) was utilized to generate multi-IF LTE-A radio frequency (RF) signals. The AWG's digital-to-analog converter (DAC) was operated to convert the digital signal to an analog signal with a 14-bit resolution and a sampling rate of 7.2 GS/s. The OMI of the optical multi-IF LTE-A signal was optically tuned by an RF attenuator and an amplifier. A commercially available direct modulation laser diode module with 3 GHz modulation bandwidth was employed as a transmitter. The generated optical signal from DML had an output of +3 dBm and transmitted over 20-km SMF. To compensate dispersion, we used the dispersion compensation fiber (DCF) having dispersion coefficient of  $-340$  ps/nm/km and an attenuation coefficient of 2.1 dB/km. The received optical power at the PIN photodiode was set to  $-10$  dBm by using a variable optical attenuator (VOA). A vector signal analyzer (VSA) was used to measure the EVM and RF spectra.

**Table 1. Parameters of the frequency plan to measure performance of intermixing noise schemes over mobile fronthaul link**

Case	Scheme	INITIAL CENTER FREQUENCY $f_i$	CARRIER SPACING $\Delta f$	Required bandwidth
Case 1: 48 IF carriers (= 59 Gb/s CPRI line rate)	IF spacing optimization	30 MHz	60 MHz	2860 MHz
	Octave-confined frequency plan	970 MHz	20 MHz	1920 MHz
	Dispersion compensation	30 MHz	20 MHz	980 MHz
Case 2: 72 IF carriers (= 89 Gb/s CPRI line rate)	IF spacing optimization	30 MHz	60 MHz	4300 MHz
	Octave-confined frequency plan	1450 MHz	20 MHz	2870 MHz
	Dispersion compensation	30 MHz	20 MHz	1460 MHz
Case 3: 144 IF carriers (= 178 Gb/s CPRI line rate)	IF spacing optimization	30 MHz	60 MHz	8620 MHz
	Octave-confined frequency plan	2890 MHz	20 MHz	5760 MHz
	Dispersion compensation	30 MHz	20 MHz	2900 MHz

The number of IF carriers used in this experiment are shown in Table 1, including the initial frequency, the IF spacing, and the total bandwidth of the transmitted signal. We measured the transmission performances for three different number of IF carriers as 48, 72 and 144. The required IF carriers at each RU is 24 to support LTE-A system with 2 carrier aggregation, 3 sector and 4 by 4 MIMO. In other words, the 144-IF carriers can cover a 6-RUs supporting a LTE-A system using a single optical wavelength. Furthermore, 144-IF carrier transmissions provides data-rates equivalent to 178 Gb/s CPRI format transmission.

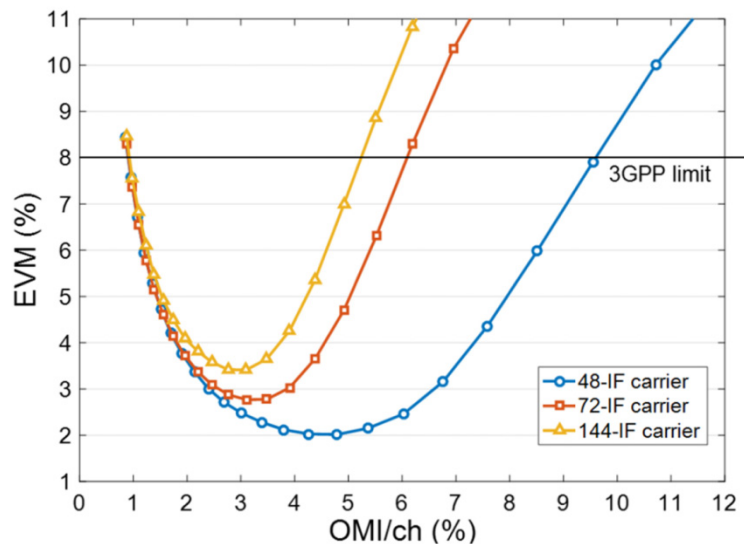


Fig. 5. EVM performance as a function of OMI/ch for 48, 72, and 144 IF carriers of the LTE-A signal under optical back to back condition.

First, we evaluate the transmission performance of multi-IF carrier of LTE-A signal in order to investigate the optimal OMI according to the number of IF carriers in the back-to-back condition (BTB) in Fig. 5. The IF spacing is set to be 20 MHz as closely spaced, and the initial center frequency of IF carrier is set to be 30 MHz. The optimal OMI/ch are shown as 3%, 3.5% and 4.5% for the 48-IF, 72-IF, and 144-IF carriers, respectively. The RF input power at the optimal OMI/ch is about  $-1$  dBm. It can be clearly observed that the noise component is the dominant EVM degradation factor at low OMI/ch. On the other hand, in high OMI/ch, the EVM is limited by the inherent nonlinearity of DML where clipping phenomenon occurs. The results show that the maximum achievable EVM are estimated to be around 2%, 2.8%, and 3.5% for 48-IF, 72-IF, and 144-IF carriers, respectively, while satisfying minimum requirement of LTE signal with 64-QAM defined by the technical specification of the 3rd generation partnership project (3GPP) [21].

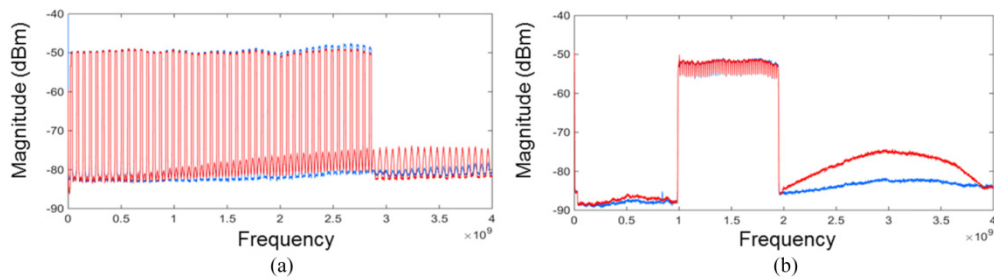


Fig. 6. Measured RF spectra of received multi-IF carriers signal under optical BTB condition (blue) and 20-km transmission (red) (a) IF spacing optimization; (b) octave-confined frequency plan.

Figure 6 shows the measured RF spectra of the received 48-IF carriers signal for IF spacing optimization and octave-confined frequency plan under optical BTB condition and 20-km transmission. It is clearly observed that the magnitude of the crosstalk caused by frequency chirp and fiber dispersion increases considerably after optical fiber transmission. In addition, it can be confirmed that the amount of second-order distortion components increases in proportional to the frequency because the intermixing noise is proportional to the square of the frequency and the square of the fiber length as Eq. (4). Therefore, we can clearly observe that the upper side intermixing noise is more dominant in Fig. 6. However, when using the IF spacing optimization technique, the overall transmission performance degradation is negligible in which the distortion components did not interfere with the desired IF carriers as shown in Fig. 6(a). It is also observed that the intermixing noise has fallen out-of-signal band without interference due to octave-confined frequency plan as shown in Fig. 6(b).

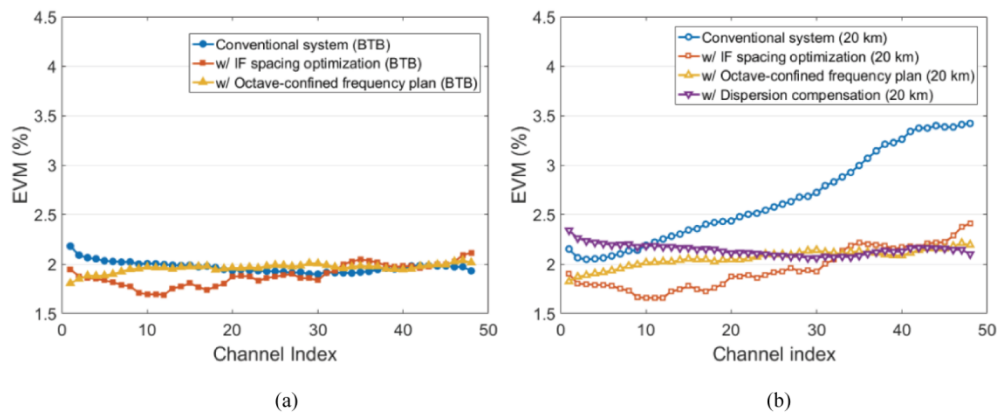


Fig. 7. EVM performances as functions of channel index for 48-IF carriers LTE-A signal under optical BTB condition and 20-km transmission with IF spacing optimization, octave-confined frequency plan, and dispersion compensation schemes (a) optical BTB; (b) 20-km transmission.

Figure 7 shows that the measured EVM performance of 48-IF carriers of the LTE-A signals for optical BTB and 20-km transmission. The RF input power is set to  $-1$  dBm. The conventional system and dispersion compensation scheme use a 20 MHz IF carrier spacing and a 30 MHz initial center frequency. In the optical back-to-back configuration, there is a slight performance difference between three schemes due to non-flat frequency response of optical transmitter [22]. Nevertheless, it is worth noting that these transmission performance variations are negligible because EVM difference is within 1%. Compared to other schemes, the IF spacing optimization causes a sufficient frequency spacing between the IF carriers. Therefore, the quantity of crosstalk between IF carriers is the lowest level in the IF spacing

optimization scheme. However, a 2.86 GHz bandwidth is required to transmit 48-IF carriers LTE-A signals using IF spacing optimization scheme. On the other hands, the required bandwidths for octave-confined frequency plan and dispersion compensation schemes are 1.95 GHz and 0.98 GHz, respectively. After 20-km transmission, the intermixing noise occurs by frequency chirp of DML and fiber chromatic dispersion, while degrading the transmission performances of data bearing multi-IF carriers. Since the intermixing noise increases in proportion to the frequency up to the sum of the first IF carrier center frequency and the last IF carrier center frequency due to second intermodulation and harmonics generations, the EVM performance of the received IF carrier is further degraded in the higher frequency band. On the other hand, when using the IF spacing optimization scheme or octave-confined mapping, the intermixing noise is generated between IF carriers as out-of-band crosstalk, in which the performance degradation would be negligible. Unlike the two schemes to avoid intermixing noise, the dispersion compensation technique could be used to suppress intermixing noise, because the interaction of the fiber chromatic dispersion and the DML chirp is a linear process before it is detected in the photodiode.

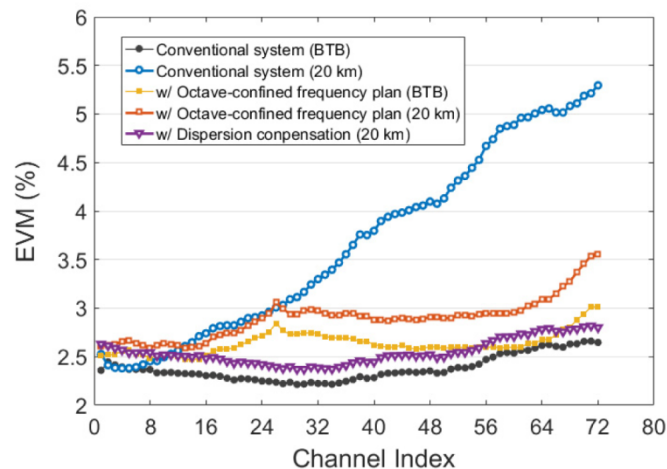


Fig. 8. EVM performances as functions of channel index for 72-IF carriers LTE-A signal under BTB condition and 20-km transmission with octave-confined frequency plan and dispersion compensation schemes.

In Fig. 8, we also show the transmission performances of 72-IF carriers LTE-A signals as a function of channel index for BTB and 20-km transmission. Because the required bandwidth to transmit the 72-IF carrier LTE-A signal using IF spacing optimization exceeds the allowable bandwidth of the conventional directly modulated laser diode, we do not employ the IF spacing optimization scheme in this experiment. It is observed that measured EVMs for the entire IF carrier under BTB conditions remain below 3%. After 20-km transmission, the measured EVM at the last IF carrier is degraded up to 5.2% due to intermixing noise. On the other hand, performance degradation caused by intermixing noise could be reduced to less than 0.5% EVM using either dispersion compensation or octave-confined frequency planning. The slight EVM degradation in scheme 2 may be caused by the dispersion-induced RF power fading of the double-sideband intensity-modulated optical signal.

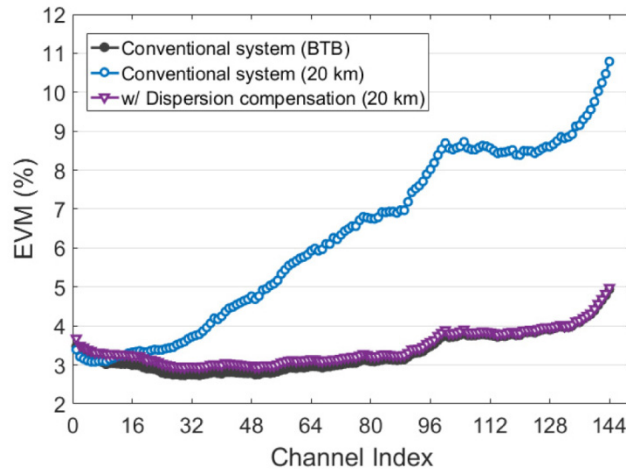


Fig. 9. EVM performances as functions of channel index for 144-IF carriers LTE-A signal under BTB condition and 20-km transmission with dispersion compensation scheme.

Figure 9 shows the EVM performance of 144 IF carriers after transmission over 20-km SMF. Because the IF spacing optimization and octave-confined frequency plan schemes do not satisfy the required 3 dB bandwidth of the commercially available directly modulated laser diode used in this experiment, the experiment is performed for dispersion compensation technique only. Due to the non-flat frequency response of the AWG and optical transmitter, a 2.5% EVM deviation is observed under optical BTB conditions. After 20-km transmission, the EVMs exceeds 8%, which is a minimum requirement for 64-QAM in 3GPP [23]. The experimental results show that the EVM performances 144-IF carriers are maintained less than 5% using dispersion compensation technique. As a results, bandwidth efficient transmission of multi-IF carrier LTE-A signal could be realized by mitigating intermixing noise in IFoF based mobile fronthaul link.

#### 4. Summary

We presented three schemes of multi-IFoF-based mobile fronthaul link to mitigate the second-order distortion induced by fiber dispersion, and also experimentally validated of these mitigation schemes. Since the dominant distortion by interaction between fiber dispersion and directly modulated laser chirp was second-order intermodulation and harmonics distortions, we were able to avoid the intermixing noise by using IF spacing optimization scheme that the carrier spacing was at least the three times the bandwidth of an IF carrier, and the initial center frequency was odd times of the half the IF carrier spacing. Alternatively, the performance degradation caused by intermixing noise could be prevented by setting initial center frequency of IF carrier as octave-confined frequency plan. Because the IF spacing optimization and octave-confined frequency plan were relatively simple methods that set the IF spacing and initial center frequency of IF carrier, it was not necessary to increase the cost and complexity for implementation. However, this advantage came at the expense of spectral efficiency loss. To improve bandwidth efficiency, we employed dispersion compensation technique in which the intermixing noise was clearly suppressed. The 144-IF carriers of the LTE-A signal equivalent to 178 Gbps CPRI line data rate were successfully transmitted over 20-km SMF using dispersion compensation technique. The experimental results showed the EVM for entire 144-IF carriers with the LTE-A signal was maintained below 6% after 20-km transmission. We believe the intermixing noise mitigation schemes could be applied to next generation mobile fronthaul link to support 5G mobile communication system.

**Funding**

This work was supported by 'The Cross-Ministry Giga KOREA Project' grant from the Ministry of Science, ICT and Future Planning, Korea.